A 19-month Record of Marine Aerosol-Cloud-Radiation Properties derived from DOE ARM AMF deployment at the Azores: Part I: Cloud Fraction and Single-layered MBL Cloud Properties

Xiquan Dong, Baike Xi, and Aaron Kennedy

Department of Atmospheric Sciences, University of North Dakota, Grand Forks, ND, USA

Patrick Minnis

Science Directorate, NASA Langley Research Center, Hampton, VA, USA

Robert Wood

Department of Atmospheric Sciences, University of Washington, Seattle, WA, USA

Revised to the *Journal of Climate* (December 17, 2013)

Corresponding author address: Dr. Xiquan Dong, The Department of Atmospheric Sciences, University of North Dakota, 4149 Campus Road, Box 9006, Grand Forks, ND 58202-9006. Email: dong@aero.und.edu. Phone: 701-777-6991.

Abstract: A 19-month record of total, and single-layered low (<3 km), middle (3-6 km), and high (> 6 km) cloud fractions (CFs), and the single-layered marine boundary layer (MBL) cloud macrophysical and microphysical properties was generated from ground-based measurements at the ARM Azores site between June 2009 and December 2010. This is the most comprehensive dataset of marine cloud fraction and MBL cloud properties. The annual means of total CF, and single-layered low, middle, and high CFs derived from ARM radar-lidar observations are 0.702, 0.271, 0.01, and 0.106, respectively. Greater total and single-layered high (> 6 km) CFs occurred during the winter, while single-layered low (< 3 km) CFs were more prominent during summer. Diurnal cycles for both total and low CFs were stronger during summer than during winter. The CFs are bimodally distributed in the vertical with a lower peak at ~1 km and a higher peak between 8 and 11 km during all seasons, except summer, when only the low peak occurs. Persistent high pressure and dry conditions produce more single-layered MBL clouds and fewer total clouds during summer, while the low pressure and moist air masses during winter generate more total and multilayered clouds, and deep frontal clouds associated with mid-latitude cyclones.

The seasonal variations of cloud heights and thickness are also associated with the seasonal synoptic patterns. The MBL cloud layer is low, warm and thin with large liquid water paths (*LWP*) and contents (*LWC*) during summer, whereas during winter it is higher, colder and thicker with reduced *LWP* and *LWC*. The cloud *LWP* and *LWC* values are greater at night than during daytime. The monthly mean daytime cloud droplet effective radius r_e values are nearly constant, while the daytime droplet number concentration N_d basically follows the *LWC* variation. There is a strong correlation between cloud condensation nuclei *CCN* concentration N_{CCN} and N_d during January-May probably due to the frequent low-pressure systems because upward motion

brings more surface *CCN* to cloud base (well mixed boundary layer). During summer and autumn, the correlation between N_d and N_{CCN} is not as strong as that during January-May because downward motion from high pressure systems is predominate. Compared to the compiled aircraft in situ measurements during ASTEX, the cloud microphysical retrievals in this study agree well with historical aircraft data. Different air mass sources over the ARM Azores site have significant impacts on the cloud microphysical properties and surface *CCN* as demonstrated by great variability in N_{CCN} and cloud microphysical properties during some months.

1. Introduction

Due to their substantial role in the Earth's radiation budget, and consequently, their effect on the Earth's climate, low-level stratiform clouds have been a topic of considerable interest since publication of the classic paper describing their physics (Lilly 1968). Low-level stratiform clouds are often defined, from the satellite perspective, as clouds with tops beneath 680 hPa (~3.3 km), and include stratus, stratocumulus and shallow cumulus (Rossow and Schiffer 1991). These low-level clouds can form within both deep and shallow marine boundary layers (MBL, defined as cloud-top heights lower than 3 km in this study). MBL clouds in the subtropical regions strongly influence the regional and global climate system (e.g., Klein and Hartmann 1993). The most extensive MBL clouds occur over the east sides of subtropical oceans, and over mid-latitude oceans under conditions of modest cold air advection during periods of equatorward flow (Klein and Hartmann 1993). A strong temperature inversion at the top of the MBL, which is maintained by large-scale subsidence combined with cold sea-surface temperatures, provides conditions favorable for MBL cloud formation (Lilly 1968). These MBL clouds are maintained by vertical mixing primarily due to the strong longwave radiative cooling at the cloud top because the radiative cooling generates turbulence to maintain an upward moisture flux (Albrecht et al. 1995; Paluch and Lenschow 1991; Rémillard et al. 2012).

MBL clouds and their interactions with aerosols are extremely important components of the climate system (Wood 2012). Their treatment in climate models is one of the largest sources of uncertainty in predicting any potential future climate change (Wielicki et al. 1995; Houghton et al. 2001; Bony and Dufresne 2005). Although many improvements have been made in the Coupled Model Intercomparison Project Phase 5 (CMIP5; Taylor et al. 2012; Klein et al. 2013; Jiang et al. 2012), MBL clouds are still a problem in climate models (e.g., Stanfield et al. 2013;

91 Dolinar et al. 2013) and numerical weather prediction (NWP) models such as the NOAA/GFS
92 (Yoo and Li 2012; Yoo et al. 2013). Because their structural and optical properties are strongly
93 dependent upon interactions between aerosol/cloud microphysics and dynamics, these intricate
94 interactions involve the formation of precipitation and its effect upon cloud dynamics, turbulence,
95 and entrainment (Wood 2012). However, there continues to be a lack of understanding of many
96 key physical links between aerosol and cloud microphysical properties. In addition, we do not
97 have sufficient observations to accurately quantify the multivariate sensitivity of precipitation to
98 cloud microphysical and macrophysical properties. Therefore, such studies are essential for the
99 evaluation of both climate and process-based numerical models.

100 The climatic importance of the microphysical and macrophysical properties of MBL
101 clouds, particularly the cloud fraction, cloud-droplet effective radius (r_e) and number
102 concentration (N_d), and liquid water content/path (*LWC/LWP*), is widely recognized. Early
103 studies found that the albedo effect of these clouds is important and leads to a strong net cooling
104 of the Earth system (Hartmann and Short 1980). Slingo (1990) used a climate model to show
105 that a modest relative increase of 15-20% in the cloud fraction coupled with a 15-20% decrease
106 in r_e and a 20-30% increase in *LWP* could balance the radiative perturbation associated with
107 doubled CO_2 concentrations. Cess et al. (1990) compared 19 GCMs and found a variety of cloud
108 feedback results, ranging from modestly negative to strongly positive because various climate
109 models have different representations of cloud microphysical and radiative properties. An
110 updated comparison by Cess et al. (1996) showed a narrowed difference with most models
111 producing modest cloud feedback. This was a result of corrections to cloud optical properties in
112 the models such as improved r_e values. Recent studies, however, indicate little narrowing in the
113 cloud feedback spread of the latest model versions (Soden and Vecchi 2011; Dolinar et al. 2013).

114 It is therefore imperative to have more accurate MBL cloud microphysical properties through
115 long-term ground-based observations so that we can improve their representation in climate
116 models.

117 The DOE Atmospheric Radiation Measurement (ARM) Mobile Facility (AMF) was
118 deployed on the northern coast of Graciosa Island, Azores, (39.09^{o}N, 28.03^{o}W) for
119 approximately 19 months (June 2009-December 2010) to study the seasonal and diurnal
120 variations of MBL clouds, and to increase understanding of their formation-dissipation processes
121 over the remote subtropical Northeast Atlantic Ocean (NEA) (Wood 2009). Long-term
122 comprehensive ground-based observations at the Graciosa Island comprise an invaluable data
123 source for investigating seasonal and diurnal variations of MBL cloud fraction and
124 macrophysical and microphysical properties, as well as their interactions with aerosols and large-
125 scale synoptic patterns. These AMF#1 (henceforth AMF) ground-based observations have
126 renewed the ground-based observations over the NEA of the 1992 Atlantic Stratocumulus
127 Transition Experiment (ASTEX, Albrecht et al. 1995), which provided a month-long record and
128 was one of the first successful deployments of millimeter radars for studying MBL clouds.

129 As the first part of a series, this paper documents fundamental statistical information about
130 seasonal and diurnal variations of (1) total and single-layered low (< 3 km), middle and high (> 6
131 km) cloud fractions, and their vertical distributions and (2) single-layered daytime MBL cloud
132 (cloud-top heights < 3 km, including stratus, stratocumulus, and shallow cumulus)
133 macrophysical and microphysical properties over the Azores during the June 2009-December
134 2010. The present work, which uses 19 months of nearly continuous ground-based cloud
135 observations, should provide the most comprehensive and reliable estimates of seasonal and
136 diurnal variations of marine cloud fraction, MBL cloud macro- and microphysical properties, and

137 influences of large-scale dynamics. The results will prove valuable dataset in advancing the
138 understanding of MBL cloud processes and properties and enabling climate/forecast modelers to
139 more fully evaluate simulations over the NEA.
140
141 **2. Datasets and large-scale synoptic patterns**
142
143 Graciosa Island is also an ideal location to study marine boundary layer (MBL) clouds
144 because it is sufficiently remote to be clear of direct continental influence (1300 km from
145 Europe). Also island effects on measurements are minimal because winds are predominantly
146 from the north and west as shown in Fig. 1. The Azores typically experiences relatively clean
147 conditions advected from the central North Atlantic that produce nearly pristine MBL clouds, but
148 periodically experience episodes of polluted air masses advected from Western Europe, North
149 Africa, and North America (see Fig. 1 of Logan et al. 2013 and Wood et al. 2013) that enrich the
150 MBL clouds with aerosols (Albrecht et al. 1995; Dong et al. 1997; Wood 2009; Wood et al. 2013;
151 Logan et al. 2013). The NEA is a region of persistent but diverse subtropical MBL clouds. As
152 illustrated in Fig. 1, subsidence from a persistent high pressure system over the Azores during
153 the summer months gives rise to relatively dry conditions (relative humidity, RH ~ 65-75%) and
154 a transition from an overcast stratocumulus regime to a broken trade cumulus regime. In contrast,
155 low pressure systems tend to be located NNW of the Azores during the winter months which
156 induce anomalous westerly winds that transported moist air masses (RH ~ 75-85%) from the
157 North Atlantic to the Azores producing more multilayered clouds and deep frontal clouds
158 associated with mid-latitude cyclones.
159 Cloud macrophysical properties such as fraction, height, thickness, and temperature are
160 taken directly from the AMF merged soundings, radar, ceilometer, and lidar measurements.
161 Primary AMF cloud observations and retrievals, and their uncertainties and references are listed

in Table 1. The centerpiece of the cloud instrument array is the 95 GHz W-band ARM Cloud Radar (WACR) (Mead and Widener 2005). The WACR operates at a wavelength of 3.15 mm in a vertically pointing mode (a beamwidth of 0.19^{o}) and provides continuous profiles (2 s temporal and 43 m vertical resolution) of radar reflectivity from hydrometeors moving through the radar field of view which allows for the identification of clear and cloudy conditions. The WACR is sensitive enough (-50 dBZ at 2 km) to detect MBL small cloud droplets and large light-moderate drizzle drops (Rémillard et al. 2012).

The cloud fraction (*CF*) is simply the percentage of radar-lidar returns that are cloudy within a specified sampling time period (e.g., month). It is given by the ratio of the number of hours when both the radar and lidar/ceilometer detected clouds to the total number of hours when all measurements (radar/lidar/ceilometer) were available. This study uses approximately 12,950 hours for all-sky samples which is 94% of all possible data during the 19-month period (for more details about the instruments up/down time, see Fig. 1 of Rémillard et al. 2012). The total cloud fraction CF_T is the fraction of time when a cloud is detected anywhere in the vertical column, the single-layered low cloud fraction CF_L is the fraction of time when low clouds ($Z_{top} < 3$ km) occur without clouds above them, the high cloud amount CF_H is determined for clouds having Z_{base} higher than 6 km with no clouds underneath, while middle clouds (CF_M) range from 3 to 6 km with no clouds either above or below. Although CF_T, CF_L, CF_M, and CF_H are computed using the same denominator (all-sky samples), CF_T does not equal the sum of CF_L, CF_M, and CF_H because CF_T includes all cloudy conditions, such as some deep convective clouds and multilayered clouds that did not satisfy our definitions of single-layered low/middle/high cloud layers. These cloud fractions should not be confused with the instantaneous hemispheric cloud fractions observed by satellite and surface observations (Dong et al. 2005).

185 Cloud-top height (Z_{top}) is derived from cloud radar reflectivity profiles while cloud-base
186 height (Z_{base}) is derived from a composite of Vaisala laser ceilometer, Micropluse Lidar (MPL),
187 and cloud radar data (Clothiaux et al. 2000; Mather and Voyles 2013). Cloud-base and -top
188 temperatures, T_{base} and T_{top}, respectively, are estimated from ARM merged soundings
189 (interpolated rawinsonde soundings with other measurements and corrections, such as
190 normalization to the total atmospheric column water vapor retrieved from the microwave
191 radiometer data) using Z_{base} and Z_{top}. Cloud physical thickness (ΔZ) is simply the difference
192 between Z_{top} and Z_{base}. The *LWP* is derived from the microwave radiometer brightness
193 temperatures measured at 23.8 and 31.4 GHz using a statistical retrieval method (Liljegren et al.
194 2001). The AMF up- and down-looking standard Eppley Precision Spectral Pyranometers (PSPs)
195 provide measurements of downwelling and upwelling broadband shortwave (SW, 0.3 to 3 μm)
196 fluxes with uncertainties of roughly 10 W m^{-2} (Long and Shi 2008).
197 The daytime microphysical and radiative properties of single-layered MBL clouds are
198 retrieved from the SW and LWP data. A δ2-stream radiative transfer model is used to compute
199 the downwelling SW flux. The retrieval scheme of Dong et al. (1997) is based on an iterative
200 approach that varies cloud-droplet effective radius (r_e) and number concentration (N_d) in the
201 radiative transfer calculations until the model-calculated solar transmission matches the
202 measured one. Dong et al. (1998) parameterized the retrieved r_e as a function of *LWP*, the solar
203 transmission, and cosine of the solar zenith angle (μ_0). The optical depths are derived from the
204 ratio of *LWP* to r_e. The retrieved and parameterized low-cloud microphysical properties have
205 been validated by in situ aircraft measurements at mid-latitude continental sites (Dong et al. 1998
206 and 2002; Dong and Mace 2003). The cloud condensation nuclei (*CCN*) concentration (N_{CCN})
207 was calculated using measurements from an optical particle counter at 0.2% supersaturation by

208 the AMF Aerosol Observation System at the Azores (Jefferson 2010; Wood et al. 2013). Notice
209 that N_{CCN} increases with increasing supersaturation ratio (Hudson and Noble 2013; Wood et al.
210 2013), while N_{CCN} at 0.2% supersaturation can represent the mean atmospheric condition.
211 Although both daytime and night N_{CCN} results are available, we only use the daytime N_{CCN} to
212 maintain consistency with the daytime MBL cloud microphysical retrievals in this study.

213 To help ensure reliable daytime cloud microphysical retrievals, the cloudy cases selected
214 in this study are single-layered and overcast low clouds that persist for approximately 2 hours
215 over the AMF site. The MBL clouds primarily include stratus and stratocumulus in addition to
216 some shallow cumulus clouds with cloud-top heights less than 3 km. Five criteria were
217 established for choosing the conditions under which daytime cloud properties can be estimated:
218 (i) only single-layer and overcast low clouds are present as determined from cloud radar-lidar
219 observations, (ii) $Z_{top} < 3$ km, (iii) $20 < LWP < 700$ g m^{-2}, (iv) $\mu_0 > 0.1$, and (v) $0.08 <$ solar
220 transmission (γ) < 0.7. The physical reasons for these five criteria are discussed by Dong et al.
221 (2000). Approximately 1,091 hours (~ 13,092 samples at 5-min resolution) of daytime data
222 satisfied the above criteria during the 19-month period.
223
224 **3. Cloud Fraction**

225 In this section, seasonal and diurnal variations of total and single-layered CFs, as well as
226 their vertical distributions are presented in Figs. 2-4. The 10 CF categories at the ARM Azores
227 site during the 19-month period are summarized in Table 2. Finally we discuss the similarities
228 and differences between this study and Rémillard et al. (2012). Four seasons are defined as
229 winter (December–February), spring (March–May), summer (June–August), and autumn
230 (September–November) in this study.

231
232 **a. Seasonal variation**

233 Monthly variations of total cloud fraction (CF_T), and single-layered low (CF_L), middle
234 (CF_M), and high (CF_H) cloud fractions during the 19-month period are illustrated in Fig. 2 and
235 summarized in Table 2. Monthly means of CF_T decrease from winter to summer, reach a
236 minimum during September, and then gradually increase from September to December with an
237 annual average of 0.702. CF_L values remain nearly constant (0.22) from Janunary to May
238 followed by a significant increase to 0.38 during June-August, and then fluctuate from 0.17 to
239 0.34 during September-December. Notice that during summer, the majority of clouds are single-
240 layered low clouds (CF_L=0.38 vs. CF_T=0.61) due to a persistent high pressure system (Fig. 2)
241 and nearly 100% inversion-topped MBLs (Fig. 5a in Rémillard et al. 2012). Multilayered clouds
242 are the majority cloud type during winter when the sum of all single-layered clouds is nearly
243 0.37 (vs. CF_T=0.8). The monthly variation of CF_H is almost the same as that of CF_T, decreasing
244 from winter to summer, but mirrors the variation of CF_L. Single-layered middle clouds occur
245 least frequently and are seasonally invariant. Annual means of CF_L, CF_M, and CF_H are 0.271,
246 0.01 and 0.106, respectively, indicating that both single-layered middle and high clouds occur
247 much less frequently than single-layered low clouds at the Azores during the 19-month period.
248
249 **b. Diurnal cycle**

250 Figure 3 shows the hourly means of CF_T and CF_L for all of the data and for winter and
251 summer separately. Hourly mean *CFs* were calculated from all samples in that local hour (such
252 as between 0100-0200 LT, presented at 0200 LT in Fig. 3) during the 19-month period. For the
253 annual and winter periods, hourly means of their CF_T and CF_L are relatively invariant. During
254 summer, however, there are strong diurnal variations in both CF_T and CF_L where the variation in

255 CF_T basically follows CF_L (Fig. 3c). For example, both *CFs* remain nearly constant from
256 midnight (0000 LT) to 1000 LT, decrease from 1100 to 1500 LT followed by an increase to 1900
257 LT, and finally level off for the remainder of the night. The annual, winter, and summer hourly
258 mean CF_T differences (ΔCF_T=*Max.*–*Min.*) are 0.041 (0.041/0.70=5.9%), 0.103 (12.9%), and
259 0.173 (27.6%), respectively. For CF_L differences, they are 0.065 (22.6%), 0.086 (40%), and
260 0.208 (56.2%), respectively. The CF_L and CF_T maxima occur during night and morning with
261 minima during afternoon. This day-night difference is most pronounced during summer which is
262 consistent with the results in Wood (2012, Fig. 8a) although his definition of low cloud amount
263 differs from that in this study. This strong diurnal variation in CF_L results from mixing driven by
264 nocturnal longwave radiative cooling at the cloud top that is not countered by solar absorption at
265 night (Albrecht et al. 1995; Paluch and Lenschow 1991; Wood 2012; Rémillard et al. 2012).
266 During the day, the absorption of solar radiation near the cloud top warms the cloud layer and
267 partially offsets the longwave radiative cooling which suppresses turbulence and cloud formation
268 within MBL.
269
270 **c. Vertical distribution**
271 Figure 4 shows the annual and seasonal mean vertical distributions of *CF* derived from
272 the ARM radar-lidar observations with a 43 m vertical resolution during the 19-month period.
273 During summer, the *CF* profile is strongly peaked at 1 km with typical *CF* values of ~0.05 above
274 2 km. A very minor secondary maximum is seen near 11 km. For the other seasons, and hence,
275 for annual mean, the *CF* vertical distributions are strongly bimodal, with primary and secondary
276 peaks at roughly 1 km and between 8 and 9 km, respectively. The winter and spring seasons
277 experience not only more middle and high clouds, but also more low clouds than other seasons

278 despite the summertime maximum in single-layered low clouds. The cold season low-cloud
279 maximum is due to increased multilayered clouds. Seasonal synoptic patterns (Fig. 1) provide
280 strong support for the results in Figs. 2-4. That is, persistent high pressure and dry conditions
281 explain more single-layered MBL clouds and fewer total clouds during summer months while
282 the low pressure and moist air masses during winter months result in more occurrences of total
283 and multilayered clouds as well as more deep frontal clouds associated with mid-latitude
284 cyclones.

285 To further investigate *CF* vertical distributions, the ARM radar-lidar-derived *CFs* have
286 been classified into 10 categories (see summary in Table 2) that represent different cloud
287 formation and dissipation processes and different large-scale dynamics. The definitions of these
288 10 categories have been discussed in detail by Xi et al. (2010). Basically, the definitions of
289 single-layered low/middle/high clouds are the same as in Fig. 32 The percentages of categories
290 1-3 in Table 2 are the same as the results in Fig. 2, while the percentages in both categories 4 and
291 6 represent cumulus or convective clouds and the percentage in category 5 is for physically thick
292 cirrus clouds. Technically speaking, categories 4-6 belong to single-layered clouds, but they do
293 not fit into the definitions of single-layered low, middle and high clouds in this study, while
294 categories 7-10 are multilayered clouds. Based on this discussion, the single-layered (sum of
295 categories 1-6) and multilayered (sum of categories 7-10) CFs are 0.468 and 0.233 for the annual
296 mean, 0.496 and 0.305 for winter, and 0.485 and 0.127 for summer. The results in Table 2
297 reveal the magnitude of the winter-summer difference in multilayered cloud CFs. Table 2 also
298 shows that there are more deep frontal clouds associated with mid-latitude cyclones and/or
299 convective clouds during winter than during summer at the Azores (category 6=0.064 and 0.007
300 for winter and summer, respectively).

d. Discussion

Rémillard et al. (2012) provided the operational status of AMF WACR, ceilometer, and MWR, as well as different types of cloud occurrences during the 19-month period at the Azores. They primarily focused on MBL clouds and investigated their cloud structural and dynamical properties, such as cumulus and stratocumulus cloud fractions and associated *LWP*, drizzle, and precipitation. In this study, we provide the statistical results of total and single-layered low, middle, and high cloud fractions, as well as their vertical distributions, but do not provide different MBL cloud types and drizzle/precipitation. There are some similarities and differences between these two studies. For example, their low clouds were defined as cloud-top heights lower than 3 km (similar to this study), but their middle and high clouds were defined as cloud-base heights above 3 and 7 km, respectively (Table 2 in Rémillard et al. 2012). Also their low, middle and high cloud occurrences (Fig. 3b in Rémillard et al. 2012) represented all cloudy conditions (both single- and multi-layer), while the monthly mean CFs in Fig. 2 are representative of single-layered low, middle and high clouds. Nevertheless, their total cloud occurrence (Fig. 3a in Rémillard et al. 2012) was nearly identical to the CF_T in Fig. 2, confirming that both studies used the same datasets and had the same total cloud fraction during the 19-month period. Although there are some overlaps between these two studies, they complement each other. Therefore the combination of these two studies will provide a more complete characterization of the marine clouds and MBL clouds at the Azores.

4. Single-layered low cloud properties

In this section, all cloud properties are derived from single-layered low clouds with cloud-top heights below 3 km and no overlying clouds. Note that in this study, these clouds are defined

as MBL clouds although they can form within both deep and shallow MBLs which differs slightly from the traditional definition. In particular, the monthly mean daytime MBL cloud macrophysical properties, such as cloud-base and -top heights and temperatures and thickness, are presented in Fig. 5, and daytime microphysical properties are presented in Fig. 7. Their corresponding daytime (and night) frequency distribution functions (PDF) and cumulative distribution functions (CDF) are illustrated in Figs. 6 and 8, respectively. Their seasonal and yearly mean, standard deviation, median, and mode values are listed in Table 3. Diurnal variations of MBL cloud macrophysical and microphysical properties are shown in Fig. 9.

a. Macrophysical properties

Monthly mean daytime MBL cloud macrophysical properties derived from the 19-month Azores dataset along with variations about the means are represented as box-and-whisker plots in Fig. 5. In each plot, bottom and top of each whisker represent the 5th and 95th percentiles of the probability distribution functions (PDF), bottom and top of each box represent 25th and 75th percentiles of the PDF, and the shorter and longer lines across each box represent the median and mean, respectively. The distribution at the far right (ANN) of each plot shows the cumulative statistics from the entire daytime dataset during the 19-month period. The average for the dataset is given by the horizontal line extending across the entire plot. Monthly mean cloud-base and -top heights (Figs. 5a and 5b) are above their annual means (Z_{base} = 1.016 km, Z_{top} = 1.575 km) from December through May followed by a significant decrease in June, and then remain below or close to their annual means until November. Cloud thickness ($\Delta Z = Z_{top} - Z_{base}$) in Fig. 5c basically follows the cloud layer variation. That is, the cloud depth, on average, is about 100 m thicker during winter and spring than during summer and autumn. These results are also

348 consistent with those in Fig. 4 where the primary frequency maxima during winter and spring
349 occur at slightly higher altitudes than those during summer and autumn. Annual mean cloud-
350 base (T_{base}) and -top temperatures (T_{top}) are 281.8 and 280.1 K, respectively. Monthly T_{base} and
351 T_{top} averages basically follow the seasonal variation of surface temperature and mirror their
352 height variations, such as being below their annual means from December to May while being
353 above the means from June to November. These results indicate that the MBL cloud layer, depth
354 and temperature are deeper, thicker and cooler, respectively, from December to May than from
355 June to November in this study. This result is consistent with estimates of the seasonal variation
356 of low clouds off the Californian coast (Lin et al. 2009).

357 Seasonal variations of cloud height and thickness in Fig. 5 are also consistent with
358 seasonal synoptic patterns (Fig. 1). In essence, the lower cloud-base and -top heights and
359 shallower cloud thickness during summer are associated with the persistent high pressure and dry
360 conditions. On the other hand, the dominant low pressure systems and moist air masses during
361 winter months result in more deep frontal clouds associated with mid-latitude cyclones, which
362 will make the MBL clouds deeper and thicker.

363 Figure 6 shows the probability distribution functions (PDF) and cumulative distribution
364 functions (CDF) of cloud macrophysical properties for both day (solid line) and night (dashed
365 line) from all 5-min samples during the 19-month period. As demonstrated in Fig. 6 and
366 summarized in Table 3, the daytime and nighttime PDFs and CDFs of the MBL cloud
367 macrophysical properties are very similar. The mean, median, and mode values of Z_{base} and Z_{top}
368 are nearly the same throughout the year, indicating a near-normal distribution of MBL cloud-
369 base and -top heights at the Azores. ΔZ has a positive skew, while T_{base} and T_{top} have a negative
370 skew. The cloud bases are nearly all below 2 km and peak at 0.8-1 km. Most cloud tops are

371 located between 1 and 2 km, although 20% of the Z_{top} values are below 1 km, and 20% are above
372 2 km. Because there are no significant differences in cloud-base and -top heights between day
373 and night, the cloud thicknesses during day and night are also nearly the same with mode values
374 of 0.2-0.4 km. Nearly 80% of the clouds are less than 1 km thick. Almost all T_{base} and T_{top}
375 values are warmer than 270 K, indicating the MBL clouds are liquid-phase clouds in this study.
376 Both T_{base} and T_{top} peak at 285-290 K and have tails toward a lower temperature (~ 270 K). The
377 rise in lower T_{top} values at night coincides with the rise in Z_{top} to values greater than 1.6 km.
378
379 **b. Microphysical properties**
380 Monthly means of the daytime cloud microphysical properties, *LWP, LWC,* r_e, N_d, and
381 optical depth (τ), as well as surface N_{CCN}, are shown in Fig. 7. Their corresponding daytime (and
382 nighttime for *LWP* and *LWC*) PDFs and CDFs are plotted in Fig. 8 and their seasonal and yearly
383 mean, standard deviation, median, and mode values are listed in Table 3. As demonstrated in
384 Figs. 7a (7b), monthly means of *LWP* (*LWC*) exceed the annual mean from April to July (for
385 *LWC* from April to September), while averages for the other months fall below the annual mean.
386 These results are also reflected in their seasonal means listed in Table 3 where the *LWP* and
387 *LWC* values during spring and summer are larger than during winter and autumn. The nighttime
388 *LWP* and *LWC* averages are about 30 g m^{-2} and 0.04 g m^{-3} larger, respectively, than their daytime
389 values throughout the year, consistent with satellite measurements (e.g., Wood et al. 2002;
390 O'Dell et al. 2008). Both the median and mode values in *LWP* and *LWC* are lower than their
391 means suggesting that there is a positive skew in *LWP* and *LWC* distributions. As illustrated in
392 Figs. 8a and 8b, there are obviously larger *LWP* and *LWC* values during the night than during the
393 day.

394 Monthly mean r_e values are nearly constant and fluctuate within 1 μm around the annual
395 mean of 12.4 μm, except for January and November when the monthly r_e means are 1.8 μm and
396 1.1 μm, respectively, below annual mean. These annual and monthly means represent typical
397 MBL cloud-droplet effective radii (e.g., Dong et al. 1997; Miles et al. 2000). As listed in Table
398 3, the annual r_e mean, standard deviation, median, and mode are 12.5, 4.6, 11.9, and 11 μm,
399 respectively. The PDF in Fig. 8 coupled with nearly identical mean, median, and mode r_e values
400 indicate a near-normal distribution of r_e with a peak at 10-12 μm. Because τ was calculated from
401 the ratio of *LWP* to r_e, its monthly means are nearly the same as *LWP* variation given nearly
402 constant r_e throughout the year. The annual mean of τ is 13.1 with peaks from 5 to 15.
403 Monthly mean N_d values fluctuate around annual mean (82 cm^{-3}) with a long tail toward
404 higher values as shown in Figs. 7d and 8d. Nearly 80% of the N_d values are less than 100 cm^{-3}.
405 The method ($\sim LWC/r_e^3$) to calculate N_d assumes a lognormal size distribution (σ_x=0.38, Miles et
406 al. 2000). With nearly constant r_e values year around, the monthly variation of N_d basically
407 follows *LWC* variation (Figs. 7b-d) except during January and November because the r_e values
408 during those two months are much smaller than the annual mean.
409 Monthly mean surface N_{CCN} values have a relatively large variation around the annual
410 mean (215 cm^{-3}) with a minimum of 129 cm^{-3} during February and a maximum of 322 cm^{-3} in
411 April. The winter (266 cm^{-3}) and spring (235 cm^{-3}) seasonal mean values are much higher than
412 their summer (193 cm^{-3}) and autumn (196 cm^{-3}) complements. Monthly variation of N_{CCN}
413 follows N_d variation during January-May due to the frequent low-pressure systems because
414 upward motion can bring more surface *CCN* to cloud base (well mixed boundary layer). During
415 summer and autumn, the correlation between N_d and N_{CCN} is not as strong as that during January-
416 May because downward motion from high pressure systems is dominant. The correlation

between N_d and N_{CCN} during the 19-month period is 0.345 with the highest correlation of 0.842 during Jan-June 2010 and lowest correlation of -0.93 during September-December 2009. The PDF of *CCN* (at 0.2% supersaturation) is similar to that of N_d with peak values ranging from 50 to 250 cm^{-3}.

Combining the daytime macrophysical properties discussed in Section 4a and listed in Table 3, we can conclude that during summer the MBL cloud layer is shallow, thin, and warm with larger *LWP* and *LWC*, whereas during winter it is deep, thick, and cold with lower *LWP* and *LWC*. Note that this conclusion is totally opposite to those at the ARM SGP site (Table 2 in Dong et al. 2005) where the low cloud layers at the SGP are deeper, thicker, and warmer with less *LWP* and *LWC* during summer than during winter. These different cloud properties may be impacted by different synoptic patterns and air masses, and/or physical processes/mechanisms. Therefore, a further study to investigate these differences is warranted.

c. Diurnal variation

Hourly mean single-layered MBL cloud macrophysical and microphysical properties are calculated from all available samples in each hour from the 19-month period and are illustrated in Fig. 9. Hourly mean Z_{base}, Z_{top}, and ΔZ are nearly constant with no significant day-night variation. Hourly mean cloud-base and -top temperatures fluctuate around their daily means within 1 K (Fig. 9b) with the lowest temperature during sunrise or early morning (~ 0600-0800 LT) and the highest temperature during late afternoon (1800 LT). These results indicate that there are no strong diurnal variations in the MBL cloud macrophysical properties at the Azores.

Strong diurnal variations, however, are seen in the cloud microphysical properties (*LWP* and *LWC*) (Figs. 9c-d). There are larger nighttime *LWP* values (140 g m^{-2}) than during the daytime (109 g m^{-2}) with a semi-diurnal cycle peaked at 0500 LT and 2100 LT, respectively.

441 Because diurnal variation in cloud thickness is small, hourly mean *LWCs* are primarily
442 determined by *LWP* values (Fig. 9d). Although the day-night *LWC* difference is small (LWC_{max} -
443 LWC_{min}=0.067 g m^{-3}), it is apparent that the *LWC* is generally greater at night than during the day.
444 This result suggests that solar absorption at the cloud top not only suppresses the turbulence
445 generated through nocturnal longwave radiative cooling at cloud top and MBL cloud formation,
446 but also reduces *LWC* (i.e., adiabaticity).

447 Therefore, we can conclude that the cloud-base and -top heights, temperatures, and cloud
448 depth, are nearly invariant. There are semi-diurnal cycles in both *LWP* and *LWC* with larger
449 values at night than during the day (Figs. 9a-d). The results of this study are very similar to
450 those derived from ship-based meteorological data during the 2008 VAMOS Ocean-Cloud-
451 Atmosphere-Land Study Regional Experiment (VOCALS-REX) over the southeast Pacific
452 Ocean (Burleyson et al. 2013). Figures 9e-h show daytime hourly mean r_e, N_d, N_{CCN}, and
453 optical depth based on available retrievals. Similar to its seasonal variation, the hourly variation
454 of r_e is also small. Hourly variation of N_d (~ LWC/r_e^3) basically follows *LWC* variation with
455 some modification by r_e. Hourly variation of N_{CCN} is also flat with low values at sunrise and
456 high concentrations in late afternoon. Notice that the ratios of N_d to N_{CCN} are greater during early
457 morning and late afternoon than near local noon, probably due to more well-mixed MBLs during
458 early morning and late afternoon and more decoupled MBLs near local noon. For cloud optical
459 depth, the diurnal variation is similar to its seasonal variation, largely following that of *LWP*.
460

461 **d. Discussion**

462 Table 4 summarizes the MBL cloud *LWC*, r_e, N_d, and N_{CCN} means retrieved from this
463 study, and measured in situ by ASTEX aircraft during June 1992. Miles et al. (2000) generated a
464 comprehensive database of MBL cloud microphysical properties derived from aircraft in situ

465 measurements during various field experiments, including ASTEX, conducted before 2000.
466 MBL cloud properties, *LWC*, r_e, and N_d, were significantly different in various field experiments
467 in different climatic regimes: means (standard deviations) of 0.18 g m^{-3} (0.14 g m^{-3}), 9.6 μm (2.4
468 μm) and 74 cm^{-3} (45 cm^{-3}). Yum and Hudson (2002) processed 17 ASTEX flights, and
469 classified them into 11 maritime and 6 continental air masses. The summarized maritime
470 (continental) cloud microphysical properties of *LWC,* r_e, N_d, and N_{CCN} (0.6% supersaturation) are
471 0.164 g m^{-3} (0.119 g m^{-3}), 8.2 μm (6.1 μm), 86 cm^{-3} (183 cm^{-3}), and 163 cm^{-3} (1023 cm^{-3}),
472 respectively. Those aircraft in situ measurements are consistent with the remotely-sensed MBL
473 cloud microphysical properties documented in this study although the aircraft data were all
474 collected during a single month, June 1992. Monthly means of daytime *LWC,* r_e, N_d, and *CCN*
475 during June are 0.25 g m^{-3}, 12.4 μm, 91 cm^{-3} and 169 cm^{-3} in this study, and agree well with
476 aircraft data.

477 Garrett and Hobbs (1995) examined two different cases: one with a clean marine air mass
478 (12 June 1995) and a second adjacent, continentally-influenced air mass (22 June 1995) near the
479 Azores using aircraft data. Hudson and Li (1995) examined the 17 June 1995 case near the
480 Azores using aircraft data and found two distinguishable air masses. Dong et al. (1997) found
481 similar MBL cloud microphysical properties retrieved from ground-based measurements for the
482 17 June case. All these results and the summarized maritime and continental cloud microphysical
483 properties in Table 1 of Yum and Hudson (2002) indicate that the continentally polluted air
484 masses can be transported to the Azores and impact MBL cloud microphysical properties. For
485 example, polluted air masses can result in higher N_{CCN}, N_d, and smaller r_e, while the clean air
486 masses have lower N_{CCN}, N_d, and larger r_e, but similar *LWC*. Different air mass sources over the

Azores significantly impact cloud microphysical retrievals and surface *CCN* as demonstrated by the great variability in N_{CCN} and cloud microphysical properties during some months.

Note that the correlation between N_{CCN} and N_d in our study is not as strong as reported in the aircraft studies discussed above because N_{CCN} was calculated at the surface in this study while N_d was retrieved in the MBL cloud layer. Without aircraft in situ measurements, it is difficult to quantitatively answer how much of the surface *CCN* can be converted to N_d, and whether or not the surface *CCN* can represent cloud base *CCN*. To validate these ground-based observations and retrievals directly, it is necessary to make comparisons between aircraft data and surface retrievals

5. Summary and conclusions

This study is the first part of a series of papers describing the climatological MBL aerosol, cloud and radiative properties at the ARM Azores site and documents the most comprehensive dataset of marine cloud fraction and MBL cloud macrophysical and microphysical properties. A 19-month record of total, and single-layered low (0-3 km), middle (3-6 km), and high (> 6 km) cloud fractions, and single-layered MBL cloud macrophysical and microphysical properties was generated from ground-based observations at the ARM Azores site between June 2009 and December 2010. This comprehensive dataset was used to examine seasonal and diurnal variations, vertical distributions as well as the impact of large-scale synoptic patterns on these MBL cloud fractions and properties. We have also compared the results in this study with other studies using aircraft in situ measurements during ASTEX. From the 19-month record of ground-based observations and retrievals, we report the following conclusions:

1) Monthly variations of total cloud fraction, and single-layered low, middle, and high cloud fractions show that CF_T and CF_H were greatest during winter, while CF_L peaked during summer. Midlevel clouds occurred least frequently and were nearly invariant over the annual cycle. Both CF_T and CF_L have more pronounced diurnal cycles during summer than during other seasons. The *CF* occurring in a given altitude band is bimodally distributed throughout the year with a lower peak at roughly 1 km and a higher peak between 8 and 11 km. During the summer, the high cloud peak is less significant than during the other seasons. There are also summer season persistent high pressure and dry weather conditions that result in more single-layered MBL clouds and less total cloudiness, while during winter the frequent low-pressure systems and moist air masses generate more total and multilayered clouds, and deep frontal clouds associated with mid-latitude cyclones. Because this study and Rémillard et al. (2012) complement each other, together they provide a more complete characterization of marine clouds and MBL clouds at the Azores.

2) Seasonal variations of cloud heights and thickness are strongly associated with seasonal synoptic patterns. For example, lower cloud-base and -top heights, and diminished cloud thickness during summer are associated with persistent high pressure and dry conditions. In contrast, predominant low-pressure systems and moist air masses during winter result in more deep frontal clouds associated with mid-latitude cyclones which make the MBL cloud layer deeper and thicker. Therefore, in terms of *LWP* and *LWC*, during the summer the MBL cloud layer is shallow, thin and warm with larger *LWP* and *LWC*, whereas during winter it is deep, thick and cold with lower *LWP* and *LWC*. Cloud-base and -top heights and temperatures, and cloud depth are nearly invariant diurnally. There are also semi-diurnal cycles in both *LWP* and *LWC* with larger values at night than during the day.

3) Monthly daytime r_e means are nearly constant and fluctuate within 1 μm of the annual mean of 12.4 μm. Monthly variation of N_d basically follows the *LWC* variation. There is a strong correlation between N_{CCN} and N_d during January-May due to the frequent low-pressure systems. During summer and autumn, the correlation between N_d and N_{CCN} is not as strong as during January-May when downward motion from high pressure systems is dominant. Although taken during different periods, the cloud microphysical retrievals in this study agree with ASTEX aircraft data. Various air mass sources over the Azores significantly impact the cloud microphysical retrievals and surface *CCN* as demonstrated by the great variability in N_{CCN} calculations and cloud microphysical properties during some months.

These results can serve as a baseline for studying MBL cloud fractions, and macrophysical and microphysical properties. These results can also serve as ground truth for validating satellite retrieved MBL cloud properties at the Azores (Xi et al. 2013). This 19-month dataset over the ARM Azores site should also provide statistically reliable estimates of monthly and diurnal variations of cloud fractions and properties for climate and numerical modelers to verify their simulated MBL cloud fractions and properties. The conclusions reached here are based only on ground-based observations, and a further validation study using coincident aircraft in situ measurements is required. Future installments of this series will report on the impact of clouds on surface and TOA radiation budgets as well as MBL aerosol-cloud interactions at the Azores.

Acknowledgments:

The data were obtained from the Atmospheric Radiation Measurement (ARM) Program sponsored by the U.S. Department of Energy (DOE) Office of Energy Research, Office of Health and Environmental Research, Environmental Sciences Division. Figure 1 was generated by Mr. Timothy Logan at UND. This study was primarily supported by the NASA CERES project at University of North Dakota project under Grant NNX10AI05G and by DOE ASR project at University of North Dakota under Grant with award number DE-SC0008468. Dr. Robert Wood was supported by DOE ASR project at University of Washington with award number DE-SC0006865MOD0002. Patrick Minnis was supported by the DOE ASR program under interagency grant, DE-SC0000991/003.

References

Albrecht, B. A., C. S. Breherton, D. Johnson, W. H. Scubert, and A.S. Frisch, 1995: The Atlantic Stratocumulus Transition Experiment-ASTEX. *Bull. Amer. Meteor. Soc.*, **76**, 1-16.

Bony, S., and J.-L. Dufresne, 2005: Marine boundary layer clouds at the heart of tropical cloud feedback uncertainties in climate models, *Geophys. Res. Lett*., **32**, L20806, doi:10.1029/2005GL023851.

Burleyson, C. D., S. P. de Szoeke, S. E. Yuter, M. Wilbanks, W.A. Brewer, 2013: Observations of the diurnal cycle of southeast Pacific marine stratocumulus clouds and precipitation. *J. Atmos. Sci.* (revised).

Cess, R. D., and Coauthors, 1990: Intercomparison and interpretation of climate feedback

578 processes in 19 atmospheric general circulation models. *J. Geophys. Res.*, **95**, 16 601-16 615.
579 Cess, R. D., and Coauthors, 1996: Cloud feedback in atmospheric general circulation models: An
580 update. *J. Geophys. Res.*, **101**, 12 791–12 794.
581 Clothiaux, E. E., T. P. Ackerman, G. G. Mace, K. P. Moran, R. T. Marchand, M. A. Miller, and
582 B. E. Martner, 2000: Objective determination of cloud heights and radar reflectivities using
583 a combination of active remote sensors at the Atmospheric Radiation Measurement Program
584 Cloud and Radiation Test Bed (ARM CART) sites. *J. Appl. Meteor.*, **39**, 645-665.
585 Dong, X., T. P. Ackerman, E. E. Clothiaux, P. Pilewskie, and Y. Han, 1997: Microphysical and
586 Radiative properties of stratiform clouds deduced from ground-based measurements. *J.*
587 *Geophys. Res.*, **102**, 23,829-23,843.
588 Dong, X., T. P. Ackerman, and E. E. Clothiaux, 1998: Parameterizations of microphysical and
589 Shortwave radiative properties of boundary layer stratus from ground-based measurements.
590 *J. Geophys. Res*. **102**, 31,681-31,393.
591 Dong, X., P. Minnis, T. P. Ackerman, E. E. Clothiaux, G. G. Mace, C. N. Long, and J. C.
592 Liljegren, 2000: A 25-month database of stratus cloud properties generated from ground-
593 based measurements at the ARM SGP site. *J. Geophys. Res*. **105**, 4529-4538.
594 Dong, X., P. Minnis, and B. Xi, 2005: A climatology of midlatitude continental clouds from the
595 ARM SGP Central Facility: Part I: Low-level cloud macrophysical, microphysical and
596 radiative properties. *J. Climate,* **18**, 1391-1410.
597 Dolinar, E., X. Dong, B. Xi, A. Kennedy, J. Jiang, P. Minnis, and H. Su, 2013: Evaluation
598 of CMIP GCMs simulated cloud fraction and TOA radiation budgets using NASA satellite
599 observations. In prep. for *JGR-atmosphere*.
600 Duynkerke, P. G., H. Zhang, and P. T. Jonker, 1995: Microphysical and turbulent structure of

601 nocturnal stratocumulus as observed during ASTEX. *J. Atmos. Sci.,* **52,** 2763–2777.
602 Garrett, T. J. and P. V. Hobbs, 1995: Long-range transport of continental aerosols over the
603 Atlantic ocean and their effects on cloud structures. *J. Atmos. Sci.*, **52**, 2977-2984.
604 Hartmann, D. L. and D. Short, 1980: On the use of earth radiation budget statistics for studies of
605 clouds and climate. *J. Atmos. Sci.*, **37**, 1233–1250.
606 Houghton, J. T. and coauthors, 2001: Climate Change 2001: The Scientific Basic. Cambridge
607 University Press.
608 Hudson, J. G. and H. Li, 1995: Microphysical contrasts in Atlantic Stratus. *J. Atmos. Sci.*, **52**,
609 3031-3040.
610 Hudson, J. G. and S. Noble, 2013: CCN and vertical velocity influences on droplet
611 concentrations and supersaturations in Clean and polluted stratus clouds. Submitted to *J.*
612 *Atmos. Sci.*, March 12.
613 Jefferson, A., 2010: Empirical estimates of CCN from aerosol optical properties at four remote
614 sites, Atmos. *Chem. Phys.*, **10**, 6855-6861, doi:10.5194/acp-10-6855-2010.
615 Jiang, J. et al. 2012: Evaluation of cloud and water vapor simulations in CMIP5 climate
616 models using NASA "A-train" satellite observations. *J. Geophys. Res.*, **117**, D14105,
617 doi:10.1029/2011JD017237.
618 IPCC 2007: Climate change 2007: The physical science basis, Contribution of working group I
619 to the fourth assessment report of IPCC. Cambridge Univ. Press.
620 Klein, S.A., and D.L. Hartmann, 1993: The seasonal cycle of stratiform clouds. *J. Clim.*, **6**, 1587-
621 1606.
622 Klein, S. A., Y. Zhang, M. D. Zelinka, R. Pincus, J. Boyle, and P. J. Gleckler, 2013: Are climate
623 model simulations of clouds improving? An evaluation using the ISCCP simulator. *J.*

624 *Geophys. Res.*, **118**(3), 1329-1342, doi:10.1002/jgrd.50141.
625 Lilly, D. K, 1968: Models of cloud-topped mixed layers under a strong inversion. *Quart. J. Roy.*
626 *Meteor. Soc.*, **94**, 292-309.
627 Liljegren, J. C., E. E. Clothiaux, G. G. Mace, S. Kato, and X. Dong, 2001: A new retrieval for
628 cloud liquid water path using a ground-based microwave radiometer and measurements of
629 cloud temperature. *J. Geophys. Res*., **106**, 14 485-14 500.
630 Lin, W., M. Zhang, N. G. Loeb, 2009: Seasonal Variation of the Physical Properties of Marine
631 Boundary Layer Clouds off the California Coast. *J. Climate*, **22**, 2624–2638.
632 Long, C. N., and Y. Shi, 2008: An automated quality assessment and control algorithm for
633 surface radiation measurements. *J. of the Open Atmos. Sci.*, **2**, 23-37.
634 Logan, T., B. Xi and X. Dong, 2013: Aerosol physical and chemical properties and their
635 interaction with CCN over the AMF-Azores facility. Submitted to *J. Geophys. Res.*
636 Martin, G. M., D. W. Johnson, and A. Spice, 1994: The measurement and parameterization of
637 effective radius of drops in warm stratocumulus clouds. *J. Atmos. Sci.,* **51,** 1823–1842.
638 Martin, G.M., D. P. Rogers, P. R. Jonas, P. Minnis, and D. A. Hegg, 1995: Observations of the
639 interaction between cumulus clouds and warm stratocumulus clouds in the marine boundary
640 layer during ASTEX. *J. Atmos. Sci.,* **52,** 2902–2922.
641 Mather, J. H. andJ. W. Voyles, 2013: The ARM Climate Research Facility: A review of
642 structure and capabilities. *Bull. Amer. Meteor. Soc.*, **94**, 377–392.
643 Mead, J. B., and K. B. Widener, 2005: W-band ARM cloud radar. Preprints, *32nd Int. Conf. on*
644 *Radar Meteorology*, Albuquerque, NM, Amer. Meteor. Soc., P1R.3. [Available online at
645 http://ams.confex.com/ams/pdfpapers/95978.pdf.]
646 Miles, N.L., J. Verlinde, and E.E. Clothiaux, 2000: Cloud-droplet size distributions in low-level
647 stratiform clouds. *J. Atmos. Sci.,* **57**, 295-311.

O'Dell C. W., F. J. Wentz, and R. Bennartz, 2008: Cloud liquid water path from satellite-based passive microwave observations: a new climatology over the global oceans. *J. Climate.* **21**: 1721–1739.

Paluch, J. R. and D. H. Lenschow, 1991: Stratiform cloud formation in the marine boundary layer. *J. Atmos. Sci.*, **48**, 2141-2158.

Platnick, S. and F. P. J. Valero, 1995: A validation of a satellite cloud retrieval during ASTEX. *J. Atmos. Sci.*, **52**, 2985-3001.

Rémillard, J., P. Kollias, E. Luke, and R. Wood, 2012: Marine boundary layer clouds observations in the Azores. *J Clim.*, **25**, 7381-7398.

Rossow, W.B., and R.A. Schiffer, 1991: International Satellite Cloud Climatology Project (ISCCP) cloud data products. *Bull. Amer. Meteor. Soc*. **72**, 2-20.

Soden, B. J., and G. A. Vecchi, 2011: The vertical distribution of cloud feedback in coupled ocean-atmosphere models. *Geophys. Res. Lett.*, **38**, L12704, doi:10.1029/2011GL047632

Slingo, A., 1990: Sensitivity of the earth's radiation budget to changes in low clouds. *Nature*, **343**, 49-51.

Stanfield, R., X. Dong, B. Xi, A. Del Genio, P. Minnis, and J. Jiang, 2013: Assessment of NASA GISSCMIP5 and post-CMIP5 Model E simulated clouds and TOA radiation budgets using satellite observations: Part I: Cloud fraction and microphysical properties. Submitted to *J. Climate.*

Stephens, G. L., and C. M. R. Platt, 1987: Aircraft observations of the radiative and microphysical properties of stratocumulus and cumulus cloud fields. *J. Climate Appl. Meteor.,* **26,** 1243–1269.

670 Taylor, K. E., R. J. Stouffer, and G. A. Meehl, 2012: An overview of CMIP5 and the experiment
671 design. *Bull. Amer. Meteor. Soc.*, **93**, 485–498.
672 Wielicki, B. A., B. R. Barkstrom, E. F. Harrison, R. B. Lee III, G. L. Smith, and J. E. Cooper
673 (1996), Clouds and the Earth's Radiant Energy System (CERES): An Earth observing
674 system experiment, *Bull. Am. Meteorol.Soc.,***77**, 853–868.
675 Wielicki, B.A., R. D. Cess, M. D. King, D. A. Randall, and E. F. Harrison, 1995: Mission to
676 planet Earth: Role of clouds and radiation in climate, *Bull. Am. Meteorol. Soc.*, **76**, 2125-
677 2153.
678 Wood R., C. S. Bretherton, and D. L. Hartmann, 2002: Diurnal cycle of liquid water path over
679 the subtropical and tropical oceans. *Geophys. Res. Lett.* **29**(23): 2092.
680 Wood, R., 2009: Clouds, Aerosol, and Precipitation in the Marine Boundary Layer (CAP-MBL).
681 Available at http://www.arm.gov/publications/programdocs/doe-sc-arm-0902.pdf?id=94
682 Wood, R., 2012: Review: stratocumulus clouds. *Mon. Wea. Rev.*, **140**, 2373-2423.
683 Wood, R., et al., 2013: Clouds, Aerosol, and Precipitation in the Marine Boundary Layer: An
684 ARM Mobile Facility deployment. Submitted to *Bull. Am. Meteorol. Soc.*.
685 Xi, B. and X. Dong, P. Minnis, and M. M. Khaiyer, 2010: A 10-year climatology of cloud cover and
686 Vertical distribution derived from both surface and GOES observations over the DOE ARM SGP
687 Site. *J. Geophys. Res.,***115**, D12124, doi:10.1029/2009JD012800.
688 Xi, B., X. Dong, P. Minnis, and S. Sun-Mack, 2013: Validation of satellite-retrieved MBL cloud
689 properties using DOE AMF measurements at the Azores. In preparation for JGR.
690 Yoo, H., and Z. Li, 2012: Evaluation of cloud properties in the NOAA/NCEP Global
691 Forecaster System using multiple satellite product. *Climate Dyn.*, 10.1007/s00382-012-
692 1430-0

693 Yoo, H., Z. Li, Y.-T. Hou, S. Lord, F. Weng, and H. W. Barker, 2013: Diagnosis and testing of
694 low-level cloud parameterizations for the NCEP/GFS using satellite and ground-based
695 measurements**.** *Climate Dynamics,* DOI 10.1007/s00382-013-1884-8.
696 Yum, S.S., and J.G. Hudson, 2002: Maritime/continental microphysical contrasts in stratus.
697 *Tellus,* **54B**., 61-73.
698
699
700
701
702
703
704
705
706 **Figures**
707
708

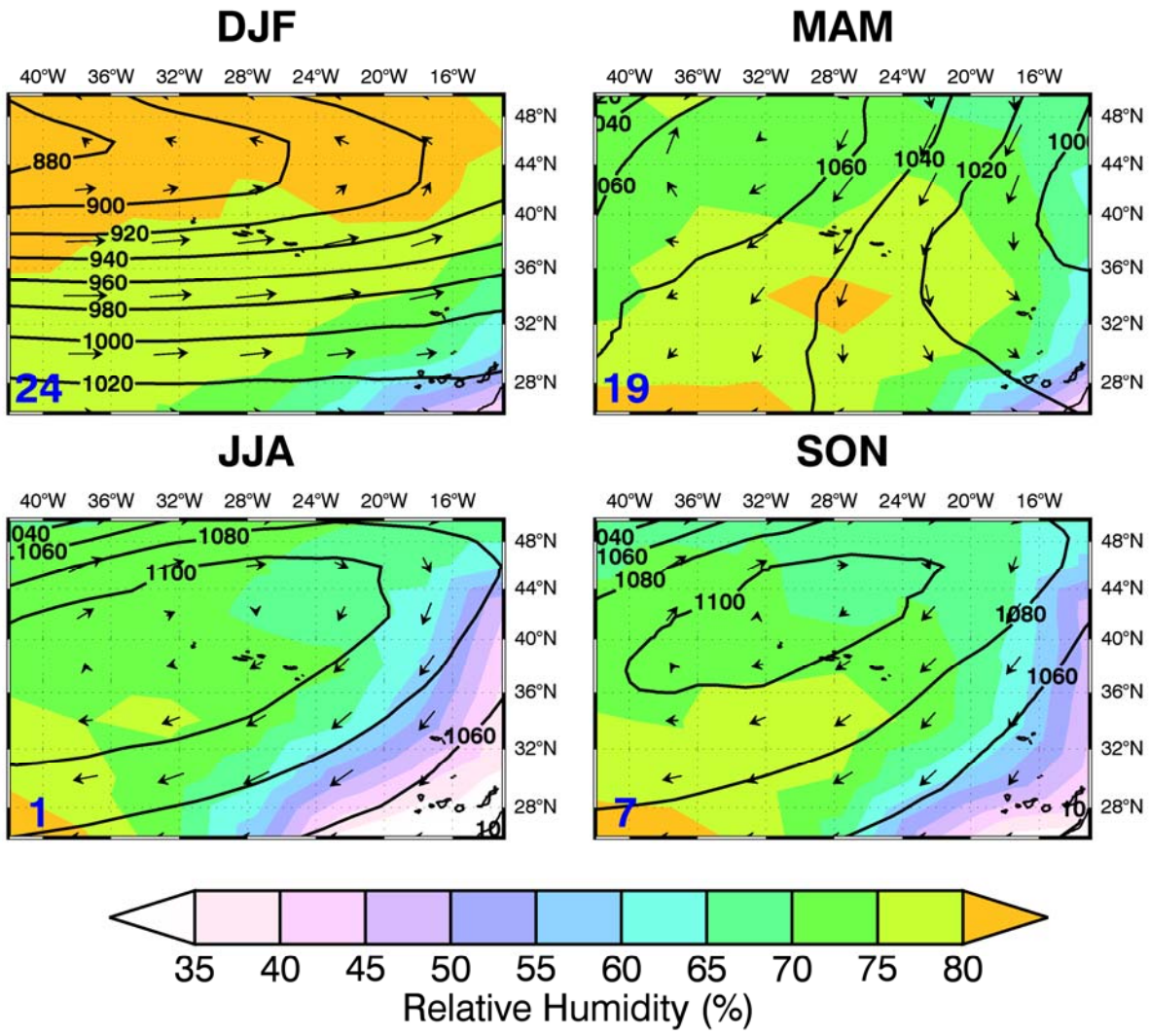

709

710 FIG. 1. 900 hPa Analysis based on the NASA MERRA reanalysis during the period June 2009-December 2010.
711 The grid box covers a range of latitudes from 26-50°N and longitudes from 42-12°W centered on the ARM Azores
712 site. Shown are 900 hPa geopotential heights, wind vectors, and shaded contours of relative humidity. The four
713 seasons are winter (DJF), Spring (MAM), summer (JJA) and Fall (SON).

714

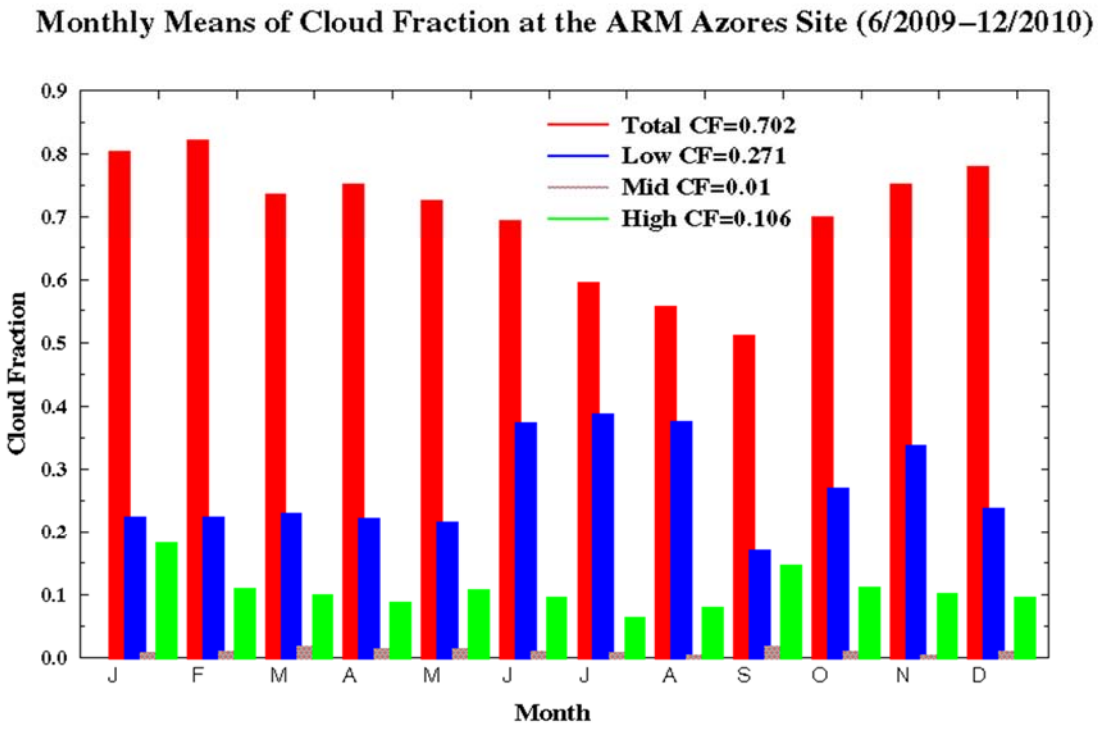

715

716 FIG. 2. Monthly mean cloud fractions derived from DOE ARM radar-lidar measurements
717 during the DOE ARM Mobile Facility (AMF) June 2009-December 2010 deployment at
718 Graciosa Island, Azores (39.09°N, 28.03°W). Total CF includes any clouds above the radar-
719 lidar instruments. Single-layered clouds: Low CF ($Z_t \leq 3$ km), Mid CF ($Z_b > 3$ km, $Z_t \leq 6$ km),
720 and High CF ($Z_t > 6$ km).

721

722

723

724

725

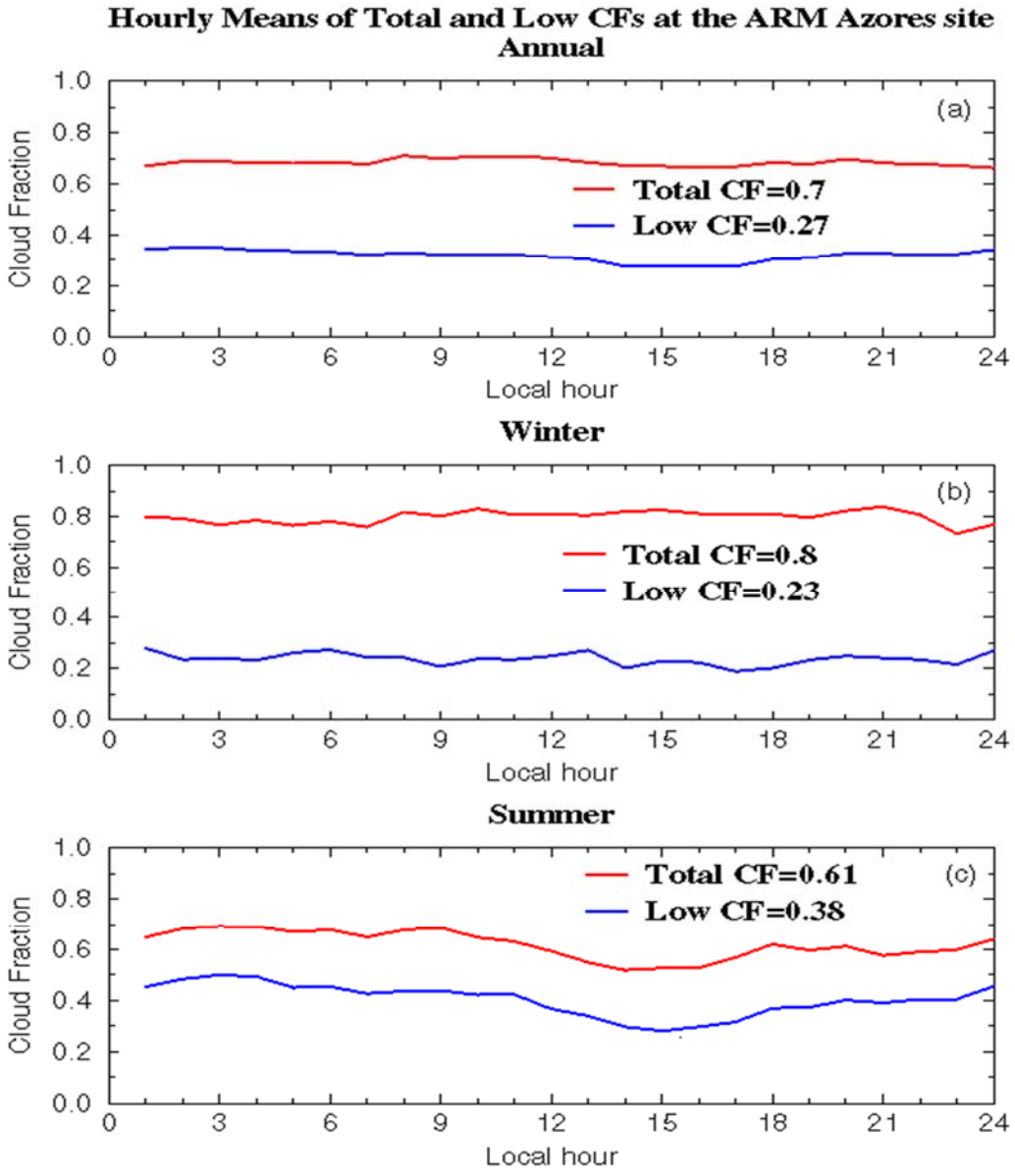

726

727 FIG. 3. Same as FIG. 2, except for hourly mean cloud fraction derived from ARM radar-lidar
728 observations at the ARM Azores site during the 19-month period. Local hour at the ARM
729 Azores site is UTC-1 hr. The means for annual, winter and summer are shown at each panels for
730 total and low cloud fractions, respectively.

731

732

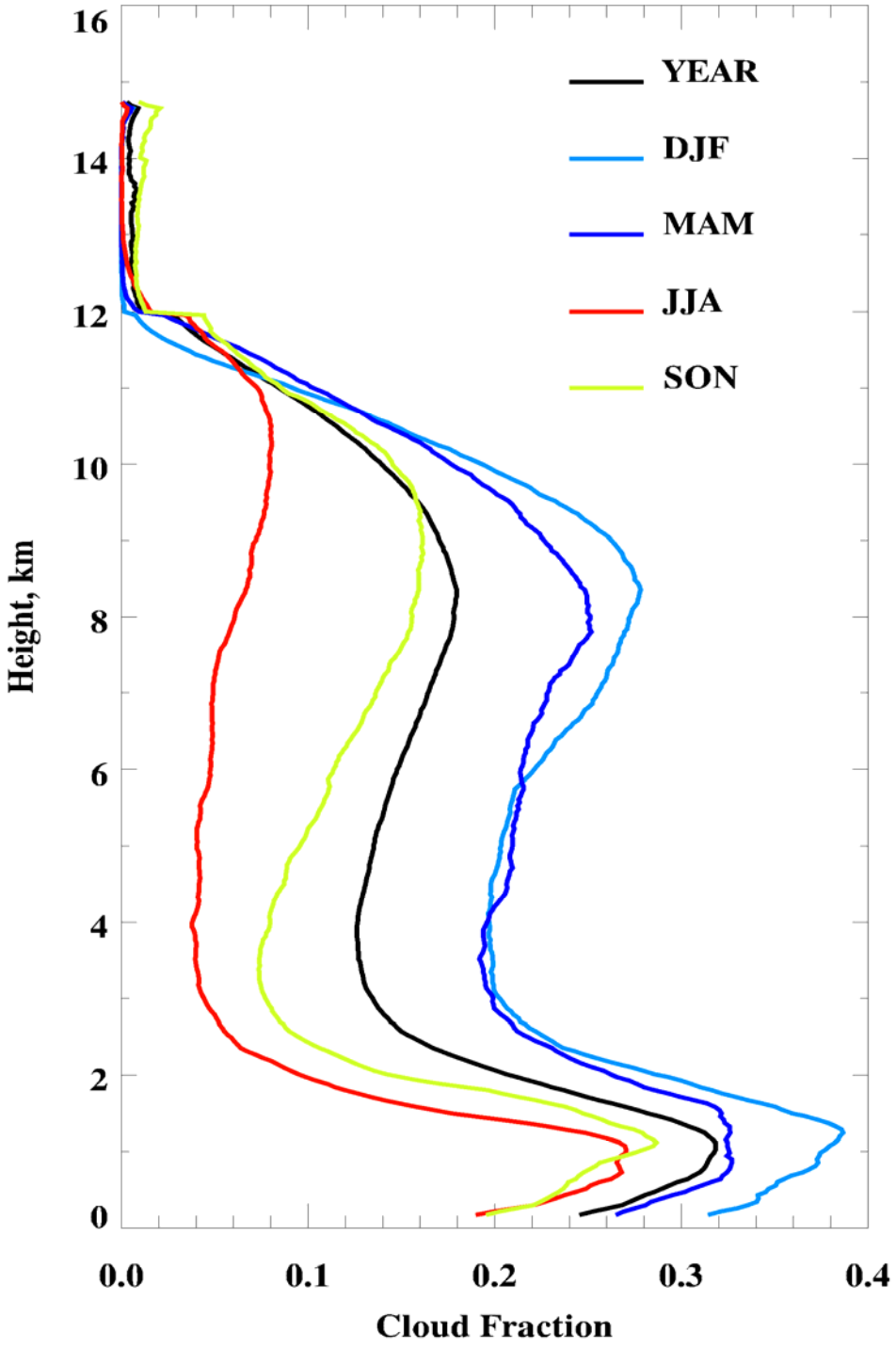

733

734 FIG. 4. Mean vertical distributions of CF derived from the ARM radar-lidar observations with a
735 vertical resolution of 43 m and a temporal resolution of 5 min at the ARM Azores site,
736 06/2009-12/2010.

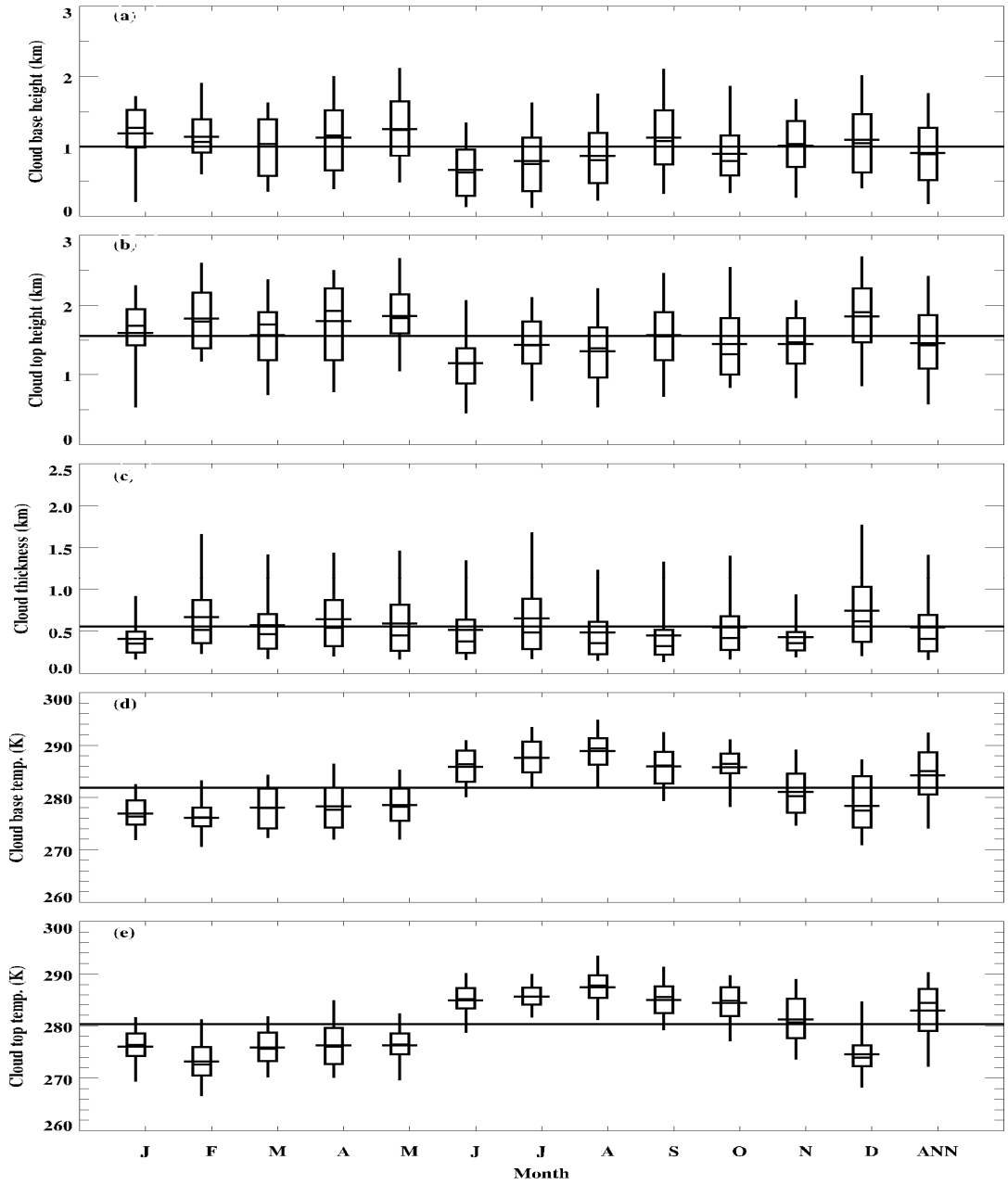

737

738 FIG. 5. Monthly mean daytime single-layered marine boundary layer (MBL) cloud
739 macrophysical properties derived from a total of 19 months ARM Azores observations. Bottom
740 and top of each whisker represent the 5th and 95th percentiles, bottom and top of each box
741 represent 25th and 75th percentiles, and the shorter and longer lines across each box represent
742 the median and mean, respectively. The distribution at the far right (ANN) of each plot shows
743 cumulative statistics derived from all daytime data sets during the 19-month period, and the
744 yearly average from entire dataset is drawn across the entire plot.

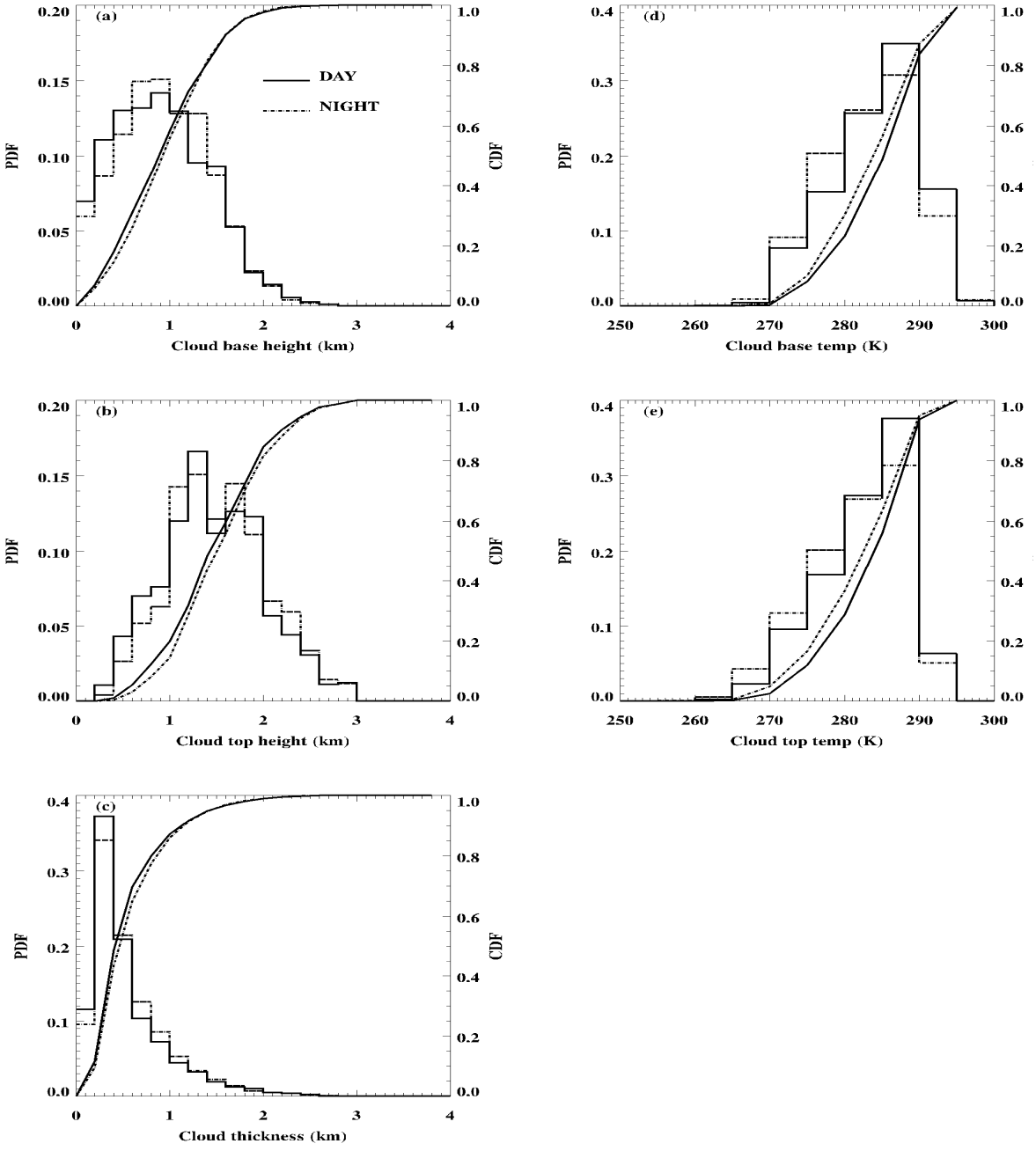

745

746 FIG. 6. Probability Distribution Functions (PDF) and Cumulative Distribution Functions (CDF)
747 of single-layered MBL cloud macrophysical properties for both day (solid line) and nighttime
748 (dashed line) from all 5-min samples at the ARM Azores site during the 19-month period.

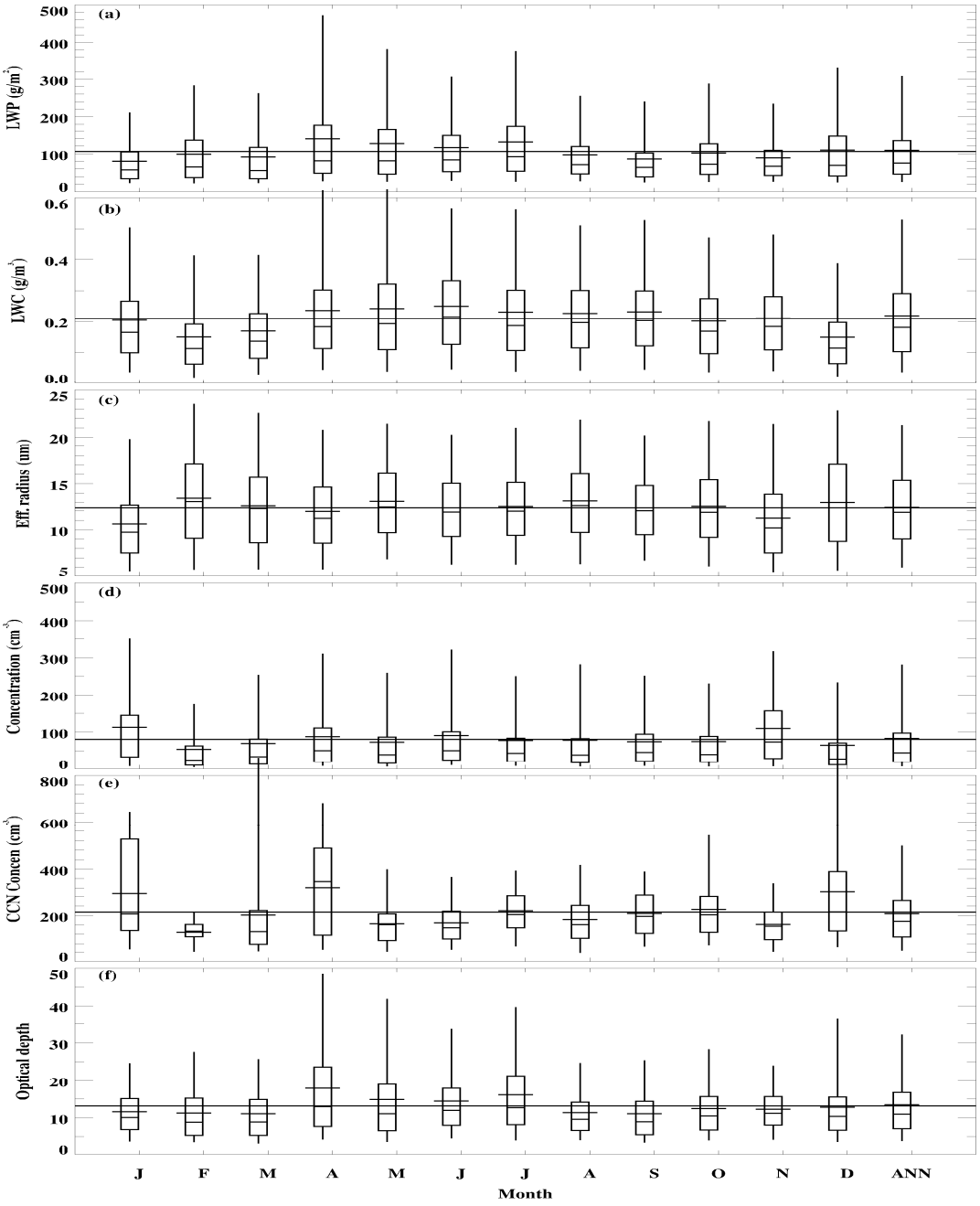

749

750 FIG. 7. Same as FIG. 5, except for daytime MBL cloud microphysical properties: (a) LWP, (b)
751 LWC, (c) cloud-droplet effective radius r_e and (d) number concentration N_d, and (f) optical depth,
752 as well as (e) surface CCN.
753

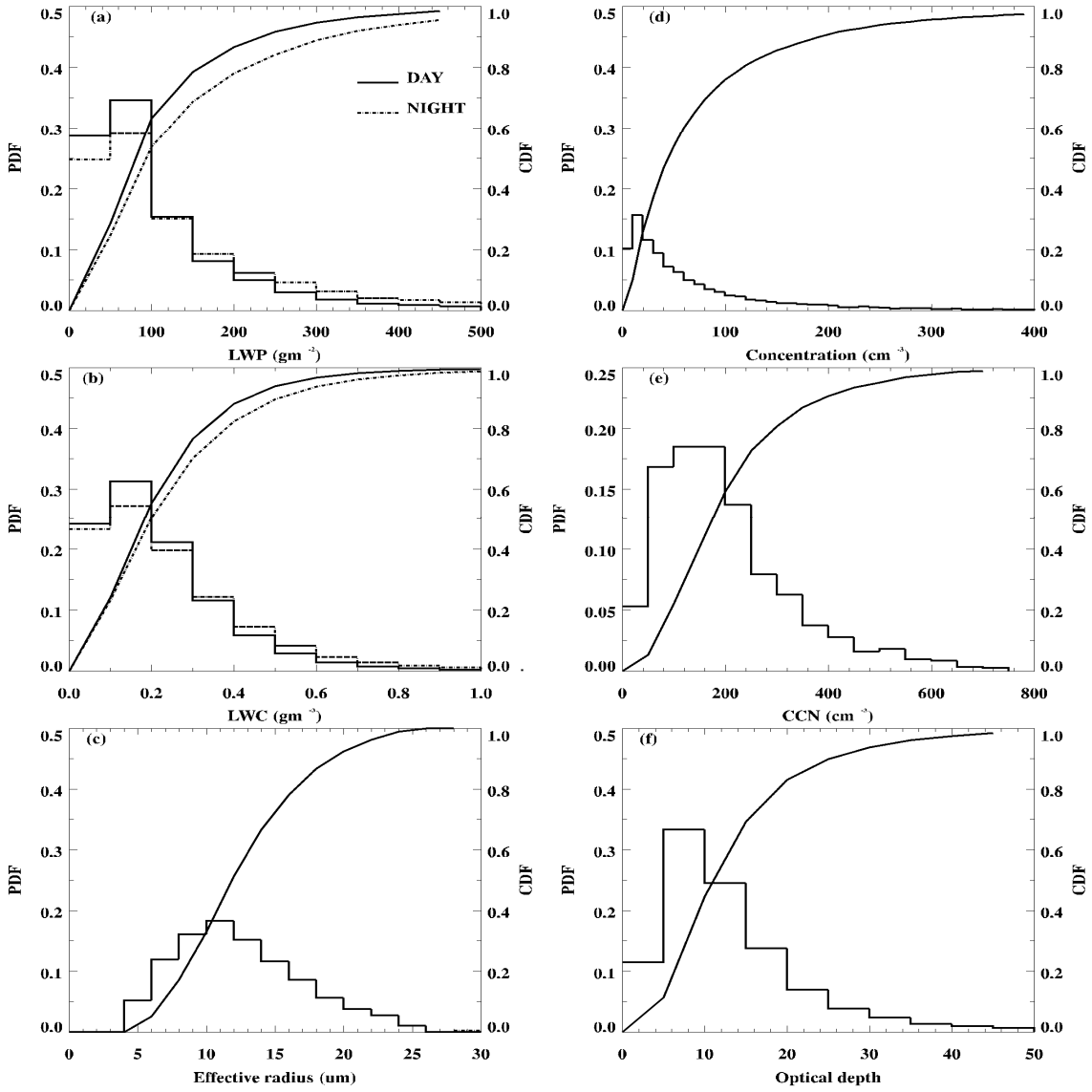

754

755 FIG. 8. Same as FIG. 6, except for MBL cloud microphysical properties and surface CCN.

756
757
758

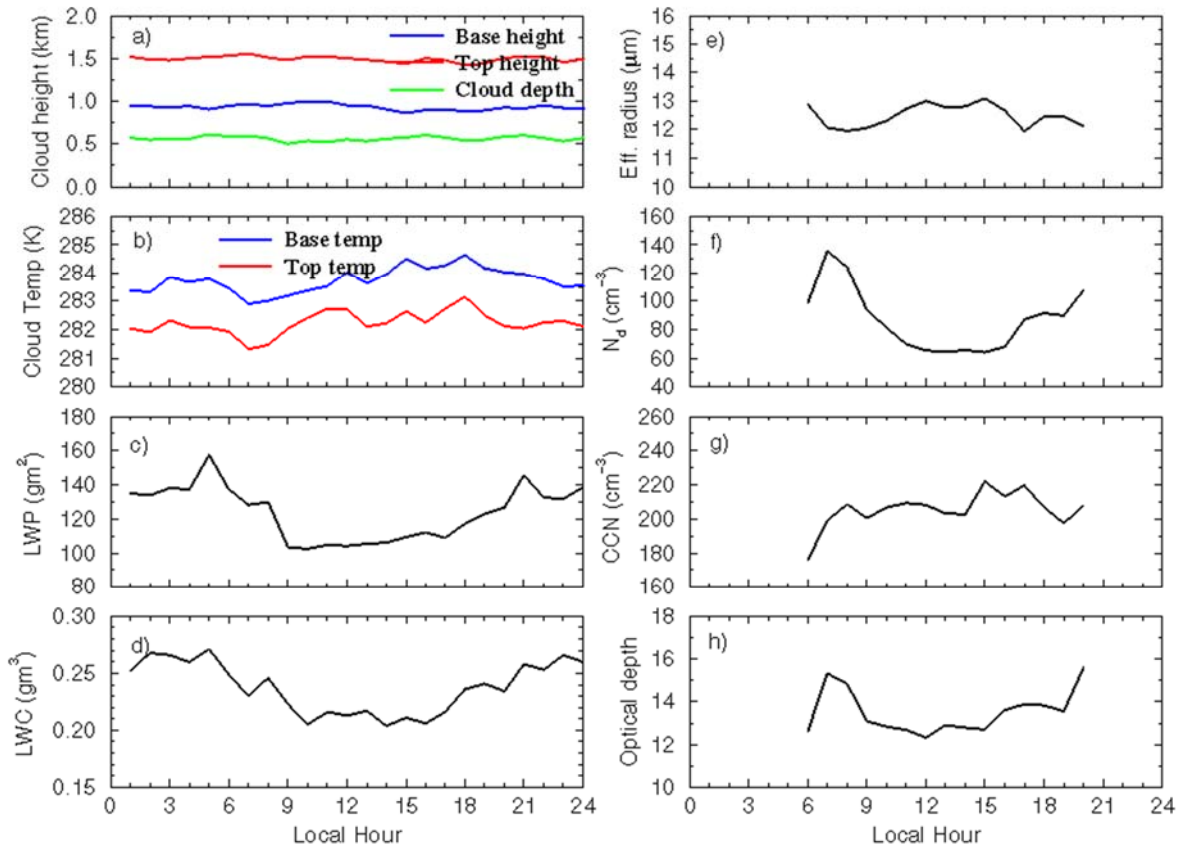

FIG. 9. Same as FIG. 3, except for hourly means of single-layered MBL clouds properties from both daytime and nighttime datasets. Only daytime r_e, N_d and optical depth, and surface *CCN* are plotted due to available retrievals.

780 TABLE 1. Cloud property measurement and retrieval methods used at AMF (Azores)

Cloud Parameter	Instruments/ Methods	Uncertainty	References
Cloud base height	Ceilometer	15 m	Rémillard et al. (2012)
Cloud base height	Micropulse lidar	30 m	Clothiaux et al. (2000)
Cloud top height	Microwave cloud radar	43 m	Rémillard et al. (2012)
Cloud base and top temperatures	Merged sounding	0.2 °C	ARM website www.arm.gov
Cloud LWP	Microwave radiometer	~20 gm^{-2} for LWP<200 ~10% for LWP >200	Dong et al. (2000); Liljegren et al. 2001
Cloud LWC	LWP/cloud thickness		
r_e	Parameterization r_e=2.07+2.49lwp+10.25γ-0.25μ_0 +20.28lwp*γ-3.14lwp*μ_0	~ 10% for daytime	Dong et al. (1997, 1998, 2002)
N_d	Parameterization $N_d = lwc/[\frac{4}{3}\pi\rho_w r_e^3 \exp(-3\sigma_X^2)]$	~ 20-30% for daytime	Dong et al. (1997, 1998, 2002)
τ	Parameterization τ=1.5*lwp/r_e	~ 10 % for daytime	Dong et al. (1997, 1998, 2002)
CCN	AMF Aerosol Observing System	~	ARM Webpage: www.arm.gov (Jefferson, A., 2010, Wood et al. 2013, Hudson and Noble 2013)
γ	SW↓(cloud)/SW↓(clear)	~ 5% for daytime	Long and Shi (2008)

781

782
783
784
785
786
787
788
789
790
791
792
793
794
795
796
797
798

TABLE 2. Summary of 10 cloud categories at the ARM Azores site (06/2009-12/2010)

Cloud type	Definition (km)	Annual	Winter	Summer
1	Single low, < 3 km	0.271	0.228	0.377
2	Single middle, 3-6 km	0.01	0.009	0.007
3	Single high, > 6 km	0.106	0.128	0.078
4	Middle over low, contiguous	0.022	0.034	0.009
5	High over middle, contiguous	0.023	0.033	0.007
6	High over both mid and low, contiguous	0.036	0.064	0.007
7	Middle over low, non-contiguous	0.02	0.028	0.011
8	High over middle, non-contiguous	0.025	0.028	0.01
9	High over low, non-contiguous	0.103	0.156	0.032
10	High over mid and low, non-contiguous	0.085	0.089	0.074
Sum	**Total CF**	**0.70**	**0.80**	**0.613**

812

813 TABLE 3. Seasonal and yearly averages, standard deviations, medians, and modes of various
814 cloud parameters derived from the 19-month ARM Azores dataset

	Winter		Spring		Summer		Autumn		Year	
	Day	Night	Day	Night	Day	Night	Day	Night	Day	Night
CF	0.231	0.215	0.215	0.212	0.352	0.370	0.259	0.284	0.282	0.295
Z_{base}, km	1.14 0.48 1.15 1.5	1.12 0.4 1.12 1.1	1.15 0.51 1.17 1.5	1.08 0.52 1.06 0.7	0.76 0.47 0.73 0.3	0.79 0.47 0.76 0.7	1.0 0.48 0.96 0.09	0.98 0.48 0.92 0.9	0.92 0.51 0.88 0.9	0.95 0.49 0.91 0.9
Z_{top}, Km	1.77 0.53 1.82 1.9	1.78 0.47 1.73 1.7	1.75 0.54 1.82 1.9	1.71 0.56 1.69 1.75	1.31 0.50 1.3 1.3	1.35 0.48 1.3 1.3	1.47 0.51 1.43 1.9	1.51 0.51 1.52 1.1	1.46 0.54 1.43 1.3	1.52 0.52 1.52 1.3
ΔZ, Km	0.63 0.45 0.49 0.4	0.66 0.4 0.55 0.3	0.6 0.42 0.48 0.3	0.63 0.46 0.49 0.3	0.55 0.43 0.4 0.3	0.56 0.42 0.42 0.3	0.48 0.34 0.37 0.3	0.53 0.36 0.42 0.3	0.55 0.41 0.41 0.3	0.58 0.41 0.45 0.3
T_{base}, K	277.2 4.5 276.4 277.5	276.7 3.8 276.6 277.5	278.3 4.4 277.9 277.5	278.5 4.8 278.5 277.5	287.4 3.9 287.7 287.5	287.3 4.0 287.5 287.5	283.8 4.9 285.0 287.5	283.2 5.2 283.8 287.5	284.3 5.7 285.1 287.5	283.2 6.0 283.8 287.5
T_{top}, K	274.7 4.5 274.6 272.5	274.2 4.7 274.5 277.5	276.2 3.9 276.1 277.5	276.1 4.4 276.4 277.5	286.0 3.5 286.0 287.5	285.8 3.6 286.3 287.5	283.1 4.8 284.1 287.5	282.2 5.2 283.1 287.5	282.9 5.8 284.3 287.5	281.7 6.2 282.8 287.5
lwp, gm^{-2}	99.0 92.0 65.7 25	147.4 144.9 90.6 25	121.8 119.9 75.2 25	138.4 133.4 87.5 75	114.4 96.3 81.4 75	148.8 129.6 100.9 75	93.3 76.9 68.7 75	124.6 115.4 84.5 75	108.7 96.0 75.4 75	139.6 129.1 91.6 75
lwc, gm^{-3}	0.16 0.14 0.12 0.05	0.23 0.21 0.17 0.05	0.22 0.18 0.17 0.15	0.24 0.18 0.19 0.16	0.24 0.17 0.2 0.15	0.29 0.26 0.23 0.16	0.21 0.15 0.18 0.15	0.25 0.19 0.2 0.16	0.22 0.17 0.18 0.15	0.26 0.22 0.2 0.16
r_e, μm	12.4 5.1 11.5 9		12.6 4.6 12.0 11		12.7 4.4 12.2 11		12.0 4.6 11.2 11		12.5 4.6 11.9 11	
N, cm^{-3}	75.4 117.7 36.3 5		76.8 113.4 40.3 15		82.5 137.9 43.5 15		89.1 110.8 52.4 15		82.6 126.2 44.1 15	
CCN, cm^{-3}	265.6 222,7 173.9 125		235.3 195.9 162.7 75		192.5 109.8 173.8 125		196.1 114.8 180.4 175		207.3 143.8 175.0 125	
τ	12.1 8.4 10.0 7.5		14.9 12.7 10.9 7.5		14.0 9.7 11.4 7.5		12.1 7.3 10.5 7.5		13.5 9.6 11.0 7.5	

815

816

817 TABLE 4. MBL cloud *LWC*, r_e, N_d and *CCN* retrieved from AMF-Azores measurements
818 in this study and measured by aircraft during ASTEX (June 1992)

Location	Air mass	*LWC* gm^{-3}	r_e μm	N_d cm^{-3}	*CCN* cm^{-3}	Source
Azores Annual mean, daytime	Maritime with periodic pollution	0.219	12.5	82.6	207.3	This study
Azores June, daytime	Maritime with periodic pollution	0.25	12.4	90.6	168.5	This study
Azores, ASTEX	Maritime	0.164	8.2	86	163	Yum and Hudson (2002)
Azores, ASTEX	Continental	0.119	6.1	183	1023	Yum and Hudson (2002)
Different IOPs	Maritime	0.18	9.6	74		Miles et al. (2000)
Azores, ASTEX	Maritime	0.15-0.35	9.5-13.4	47		Albrecht et al. (1995)
Azores, ASTEX	Nocturnal stratus	0.01-0.37	5.8-9.8	100		Duynkerke et al. (1995)
Azores, ASTEX	Sc	0.15	10.8	50		Martin et al. (1994 and 1995)
Azores, ASTEX	Maritime		9.4-13.9			Platnick and Valero (1995)
Azores, ASTEX June 12	Maritime	0.23	7.3	174	30-100	Garrett and Hobbs (1995)
Azores, ASTEX June 22	Continental	0.21	5.3	457	100-800	Garrett and Hobbs (1995)
Azores, ASTEX June 17	Continental	0.2	5.4	220	668	Hudson and Li (1995)
Azores, ASTEX June 17	Maritime	0.2	12.2	35	116	Hudson and Li (1995)
Off east coast of Australia	Maritime	0.16	11.6			Stephens and Platt (1987)

819

820

821

822

823